Journal of Engineering and Sustainable Development
Vol. 30, No. 04, July 2026
https://jeasd.uomustansiriyah.edu.iq/index.php/jeasd
ISSN 2520-0917
Research Article
https://doi.org/10.31272/jeasd.2621

Torsional Performance of Reinforced Concrete Beams Strengthened with High-Performance Concrete: Numerical Analysis

Maher K. Abbas[1*], Mustafa Kareem Hamzah[2], Zahraa A. Naser[3], Nabeel H. Al-Salim[4]

[1]Department of Civil Engineering, College of Engineering, University of Warith Al-Anbiyaa, Karbala, Iraq
[2]Department of Civil Engineering, College of Engineering, Al-Qasim Green University, Babylon, Iraq
[3]Department of Civil Engineering, College of Engineering, University of Kerbala, Karbala, Iraq
[4]Department of Civil Engineering, College of Engineering, University of Babylon, Babylon, Iraq

[*]Email: eng.maher.abbas@gmail.com

Article Info

Received	**25/04/2024**
Revised	**04/05/2026**
Accepted	**15/05/2026**

Abstract

A numerical investigation of the torsional strength of composite materials using normal-strength concrete (NC) and high-performance concrete (HPC) has recently attracted researchers' attention. NC and HPC are commonly used in construction due to their mechanical properties and durability. This work evaluates the effect of strengthening RC beams with HPC to overcome severe torsional damage. To achieve the objectives, a numerical simulation of RC solid and hollow beams subjected to torsion and strengthened with HPC has been performed using three techniques: bottom, side, and U-shaped strengthening, with varying thicknesses. A constitutive model based on the ACI code (318-19) has been derived to validate the FE simulation and describe the effect of strengthening on torsional performance. The results showed that the U-shape method was the most effective and is recommended as a rehabilitation technique. The work also introduced a refined formulation, with principal tensile stress coefficients that averaged 15.2% higher than those in the ACI code. The constitutive model validated the numerical results, showing a maximum variation of less than 7% from the FE results and high R^2 values near 1, indicating a strong predictive model for torsional strength.

Keywords: Finite Element, High Performance Concrete, Numerical Analysis, Strengthening, Torsional Behavior.

1. Introduction

The torsional strength of reinforced concrete beams is crucial to ensuring the structural integrity and safety of buildings and infrastructure [1]–[3]. Numerous concrete structures, including bridge components, horizontally curved members, eccentrically loaded beams, spandrel beams, and spiral staircases, are often subjected to significant applied torque. This torque can increase loading, which in turn may cause structural damage or deterioration in these elements. To mitigate these effects, it is essential to enhance the torsional capacity of reinforced concrete beams [4]. To address this need, various strengthening techniques have been developed and employed. One common approach is the use of polymer fiber jacketing, which involves wrapping the beams with high-strength materials to improve their torsional resistance. Among these materials are Fibre-Reinforced Polymers (FRP), Carbon Fibre-Reinforced Polymers (CFRP), Glass Fibre-Reinforced Polymers (GFRP), and aramid fibers. Another effective method is ferro-cement jacketing, which involves encasing the concrete beams in a thin layer of cement mortar reinforced with wire mesh [5]–[8]. Traditionally, measures such as enlarging the section have been employed to prevent torsional failure in concrete beams [9]–[12]. However, in recent years, there has been growing interest in using ultra-high-performance concrete (UHPC) to strengthen reinforced concrete beams [13]–[18].

Numerous studies have been conducted on the strengthening of concrete beams under torsional loads [19]–[21]. These studies have shown promising results, indicating that the torsional strength of reinforced concrete beams can be significantly improved by strengthening them with high-performance concrete (HPC) [22], [23]. Mohammed et al. [11] evaluated the effectiveness of using ultra-high-performance fiber concrete (UHPFC) as external transverse reinforcement for reinforced concrete beams, with or without stirrups, subjected to pure torsion. The experimental results demonstrated that UHPFC wrapping increases the torsional moment-carrying capacity of

RC beams, with a greater increase observed for thicker UHPFC layers. The main findings include the effectiveness of UHPFC in strengthening beams, the increase in torsional moment-carrying capacity due to UHPFC wrapping, and the correlation between ultimate torque and the thickness of the UHPFC wrapping. Mohammed et al. [24] explored the effectiveness of UHPFC jacketing techniques in enhancing the torsional performance of reinforced concrete beams. The application of a thin layer of UHPFC on RC beams increased the cracking torque and improved torsional capacity in all cases, with fully wrapping the beam cross-section with UHPFC significantly increasing the ultimate torsional strength. The work concluded that UHPFC jacketing is a promising technique for the torsional upgrading of RC beams. UHPFC jackets enhance the torsional performance of RC beams, and full wrapping with UHPFC significantly increases the ultimate torsional strength. Zhou et al. [12] systematically investigated the effects of various variables on the torsional behavior of UHPC-strengthened RC beams. They compared the effectiveness of torsional strengthening with UHPC wrapping against that of FRP. The work reported that the UHPC-based strengthening strategy resulted in significantly higher cracking and ultimate torsional moments, exhibited advantages over the FRP-based technique, but led to a larger beam cross-section after strengthening.

Nevertheless, UHPC is far superior to conventional concrete in compression and tensile strength, as well as in other mechanical properties. Despite the abundant benefits of UHPC, its widespread acceptance remains hampered by its high cost. This is because reliable production requires advanced techniques and stringent quality control [12], [17]. To address this problem, this work, supported by numerical analysis, pursues two main objectives: first, to demonstrate that HPC with a compressive strength of 65 MPa is a valid and effective strengthening layer; and second, to develop a mathematical model to determine the torsional capacity of both accurately strengthened solid and hollow cross-sectional RC beams under equilibrium torsion.

2. Methodology

To predict the torsional behavior, a total of 38 solid and hollow cross-sectional beams were meticulously modeled in this work. These beams featured two distinct concrete categories: normal-strength concrete (NC) with a compressive strength of 35 MPa, used as a strengthened core, and high-performance concrete (HPC) with a compressive strength of 65 MPa, used as a strengthening layer extending the full length of the beam. The configuration and dimensions of these specimens are comprehensively outlined in Table 1 and depicted in Fig. 1.

In ABAQUS, torsion can be represented using various techniques, each offering unique advantages depending on the objectives of the work. Cao et al. [25] used a method in which the torque is applied directly by drawing a torque arm, providing a clear representation of the applied load's effect on the structure. Another approach, demonstrated by Eltaly et al. [26], involves simulating a steel box at each end of the beam and applying a moment to this box, thereby inducing torsion. This method provides a detailed understanding of the interaction between the beam and the steel box, which is particularly useful in complex scenarios, such as reinforced-concrete box girders with openings.

In this work, a simpler yet effective method was adopted. Torsion was simulated by applying a coupling constraint at both ends of the beam, thereby allowing rotation. This rotation, applied in both clockwise and counterclockwise directions, accurately depicts the torsional performance of the beam under supported boundary conditions. Additionally, to systematically examine the influence of high-performance concrete and its thickness, the beams were categorized by the position and thickness of the reinforcing layer, denoted as a position-thickness code. For example, RBL-5 indicates that a 5 mm HPC layer is attached to the right, bottom, and left sides of the beam body. Flexural reinforcement consisted of 2-φ16 mm bars at the top, middle, and bottom with a yield strength of 420 MPa, while shear reinforcement was provided by φ10 mm bars spaced at 250 mm intervals with the same yield strength. This categorization and detailing of the specimens are also presented in Table 1.

Table 1. Layer thickness and configuration of solid and hollow cross-sectional beams.

Beam Code (1) solid + (1) hollow	Layer thickness (mm) HPC
NC	---
B-50	
RL-50	50
RBL-50	
B-60	
RL-60	60
RBL-60	
B-70	
RL-70	70
RBL-70	
B-80	
RL-80	80
RBL-80	
B-90	
RL-90	90
RBL-90	
B-100	
RL-100	100
RBL-100	

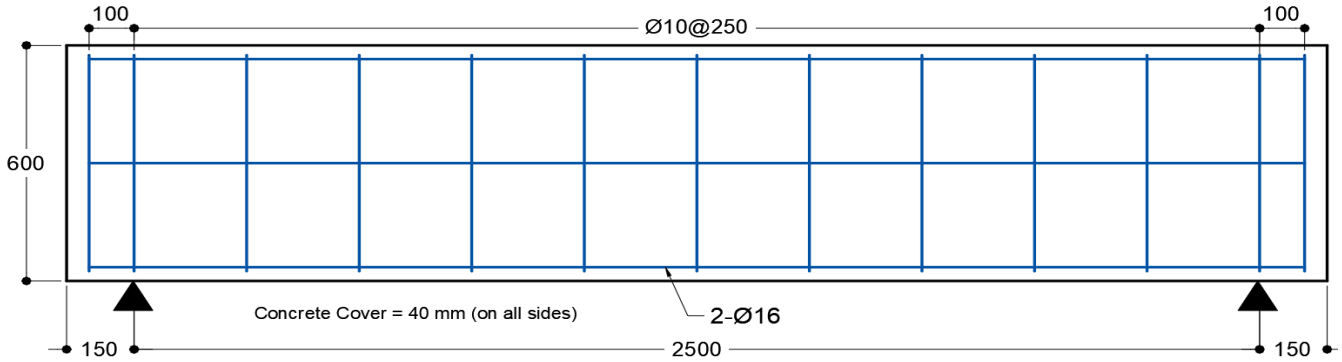

a)

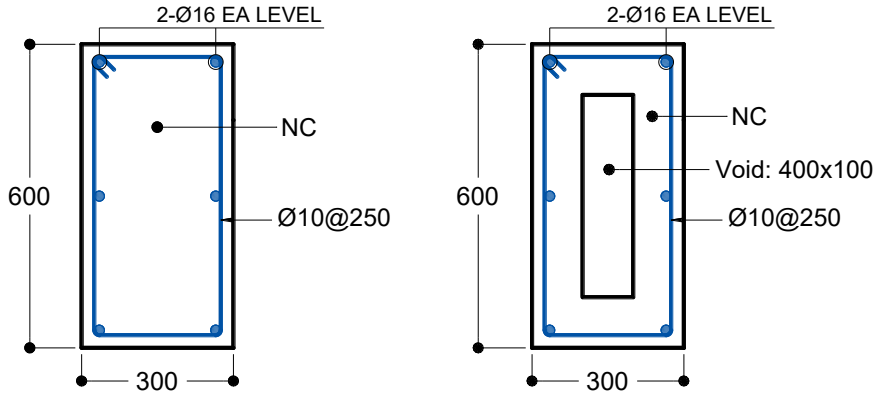

b)

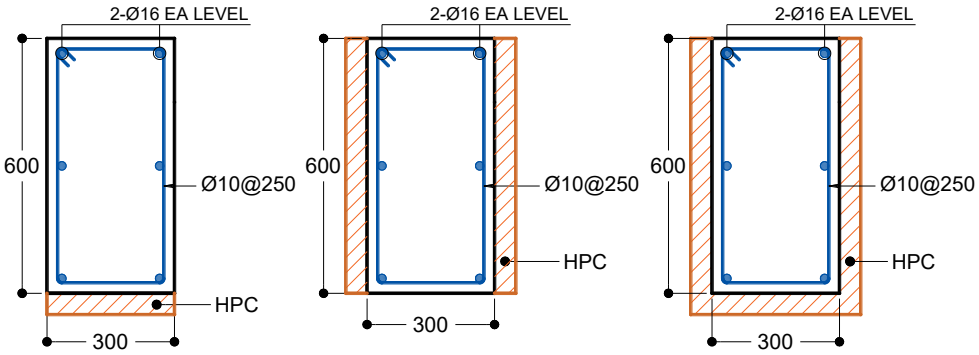

c)

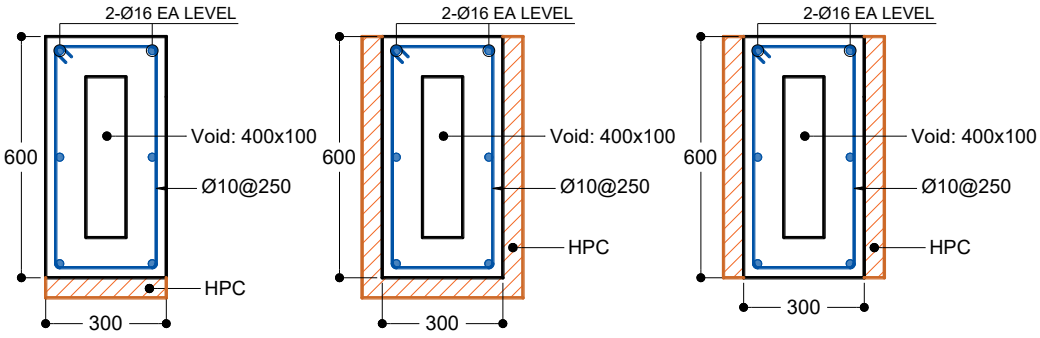

d)

Figure 1. Geometry and details of concrete beams (units: mm): a) longitudinal reinforcement, b) Control beams, c) Cross-sections of strengthened solid specimens, and d) Cross-sections of strengthened hollow specimens.

3. Finite Element Modeling

The aforementioned reinforced concrete beams were modeled and analyzed using nonlinear FE software (ABAQUS). To complete the full finite element models of the reinforced concrete beams, various numerical steps were implemented sequentially. The steps began with creating the parts, such as concrete, reinforcement, and additional HPC to be attached to the beam, using different techniques for strengthening. Then, the material properties were defined. The steel reinforcement was simulated with a 2-node linear 3D truss (T3D2), featuring an elastic modulus of 200 GPa, a Poisson's ratio of 0.3, a yield stress of 420 MPa, and an ultimate stress of 460 MPa. The concrete was modeled using an 8-node linear brick, reduced-integration (C3D8R), with an elastic modulus of 26.5 GPa and a Poisson's ratio of 0.15 for 35 MPa NC, and an elastic modulus of 37.6 GPa and a Poisson's ratio of 0.19 for 65 MPa HPC [27]. The concrete damage plasticity for both types is illustrated in Tables 2 and 3. After that, the concrete and steel sections were created and assigned to the newly created parts. Next, the NC beams and the strengthened beams were assembled. As the beam is supported, the boundary conditions are assigned to be pin and roller supports. To simulate beam torsional behavior, various techniques can be used in ABAQUS.

Table 2. Concrete damage plasticity for 35 MPa concrete.

Plasticity	**Dilation angle**	**Eccentricity**	**fb0/fc0**	**K**	**Viscosity parameter**
	35	0.1	1.16	0.667	0.01
	Compression behaviour			Tensile behaviour	
yield stress	inelastic strain	damage parameter	yield stress	cracking strain	damage parameter
12.62825	0	0	3	0	0
20.40615	0.00031	0	1.94175	0.00013	0.44522
26.90333	0.00062	0	1.37567	0.00026	0.60695
31.57123	0.00094	0	1.07725	0.0004	0.69221
34.20891	0.00125	0	0.89114	0.00053	0.74539
35	0.00156	0	0.7632	0.00066	0.78194
33.91523	0.00187	0.03099	0.66948	0.00079	0.80872
31.15215	0.00219	0.10994	0.59764	0.00092	0.82924
27.53104	0.0025	0.2134	0.54071	0.00105	0.84551
23.73333	0.00281	0.3219	0.49439	0.00119	0.85875
20.17613	0.00312	0.42354	0.45592	0.00132	0.86974
17.04726	0.00343	0.51294	0.42341	0.00145	0.87902
14.38995	0.00375	0.58886	0.39556	0.00158	0.88698
12.17461	0.00406	0.65215	0.37141	0.00171	0.89388
10.34347	0.00437	0.70447	0.35026	0.00185	0.89993
8.8336	0.00468	0.74761	0.33156	0.00198	0.90527
7.5871	0.00499	0.78323	0.31491	0.00211	0.91003
6.55451	0.00531	0.81273	0.29998	0.00224	0.91429
5.69509	0.00562	0.83728	0.2865	0.00237	0.91814
.97599	0.00593	0.85783	0.27428	0.00251	0.92163
4.37088	0.00624	0.87512			
3.85878	0.00656	0.88975			
3.42293	0.00687	0.9022			
3.04996	0.00718	0.91286			
2.72909	0.00749	0.92203			
2.45165	0.0078	0.92995			

Table 3. Concrete Damage Plasticity for Concrete of 65 MPa.

Plasticity	Dilation angle	Eccentricity	fb0/fc0	K	Viscosity parameter
	36	0.1	1.16	0.667	0
Compression behaviour			Tensile behaviour		
yield stress	inelastic strain	Damage parameter	Yield stress	cracking strain	Damage parameter
25.02	0	0	6.5	0	0
35.88	0.00034	0	3.60	0.00019	0.44522
46.35	0.00068	0	2.55	0.00039	0.60695
55.66	0.00101	0	2.01	0.00058	0.69221
62.44	0.00135	0	1.65	0.00077	0.74539
65	0.00169	0	1.41	0.00097	0.78194
61.52	0.00203	0.05343	1.24	0.00116	0.80872
52.01	0.00237	0.19977	1.11	0.00135	0.82924
39.89	0.00271	0.38629	1.01	0.00154	0.84551
28.69	0.00304	0.55858	0.92	0.00174	0.85875
20.01	0.00338	0.69221	0.84	0.00193	0.86974
13.84	0.00372	0.78705	0.78	0.00212	0.87902
9.63	0.00406	0.85183	0.73	0.00232	0.88698
6.78	0.0044	0.89564	0.69	0.00251	0.89388
4.85	0.00474	0.92539	0.65	0.0027	0.89993
3.52	0.00507	0.94582	0.61	0.0029	0.90527
2.59	0.00541	0.96004	0.58	0.00309	0.91003
1.94	0.00575	0.9701	0.55	0.00328	0.91429
1.47	0.00609	0.97732	0.53	0.00348	0.91814
1.13	0.00643	0.98258	0.51	0.00367	0.92163
0.88	0.00676	0.98646			
0.69	0.0071	0.98937			
0.55	0.00744	0.99156			

Also, there are multiple ways to represent the torsion in the literature. However, the beam's torsional performance in this work is simulated, as shown in Fig. 2.

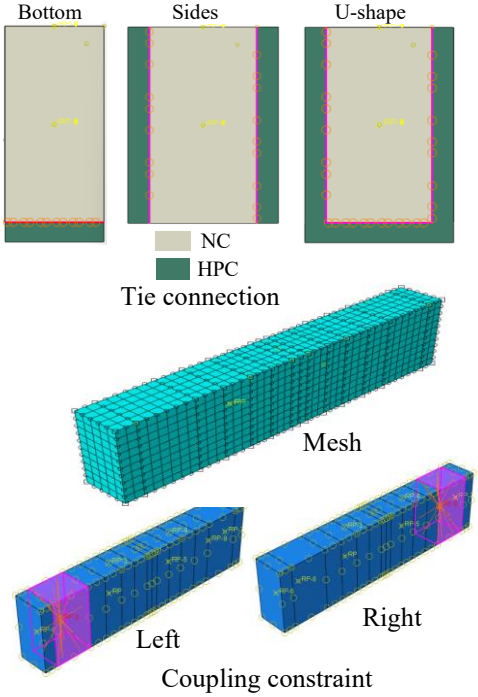

Figure 2. FEM process for the considered beam.

A coupling constraint is applied at the left and right ends of the beam, and rotation is then applied to both sides, clockwise and counterclockwise, to depict the torsional performance. The high-performance concrete is attached to the beam using a tie constraint with perfect bonding to avoid sliding. The meshing process started by assigning a seed to each part with the same element size. The first trial size was 150 mm, then 100 mm, noticing a considerable change in the results. After that, the element size was reduced to 50 mm, resulting in a significant change in the results. Subsequently, a smaller element size (25 mm) was considered, which led to an almost negligible change in the results but increased the analysis time by more than tenfold. Therefore, 50 mm was the most suitable element size and was considered in this work.

4. Results and Discussion

4.1 Finite Element Results

The cracking and damage are illustrated in Fig. 3. For the control specimens, cracks appeared immediately after applying the torque, consistent with the expected crack pattern. The damage occurred at the edges in opposite directions, indicating the need for strengthening to withstand severe torsional loads. Moreover, the solid beam exhibited greater torsional strength than the hollow beam, indicating the importance of cross-section geometry in the overall torsional behavior of the beam. Also, the aforementioned figure demonstrates cracking and damage in high-performance concrete under higher torsion.

Generally, the results indicated that HPC strengthening will enhance the torsional performance of the reinforced concrete beam. However, the cracking pattern and the location of damage are nearly the same as in the control beam, with improved capacity. The bottom strengthening technique showed the least incremental torsional capacity compared with the other rehabilitation techniques.

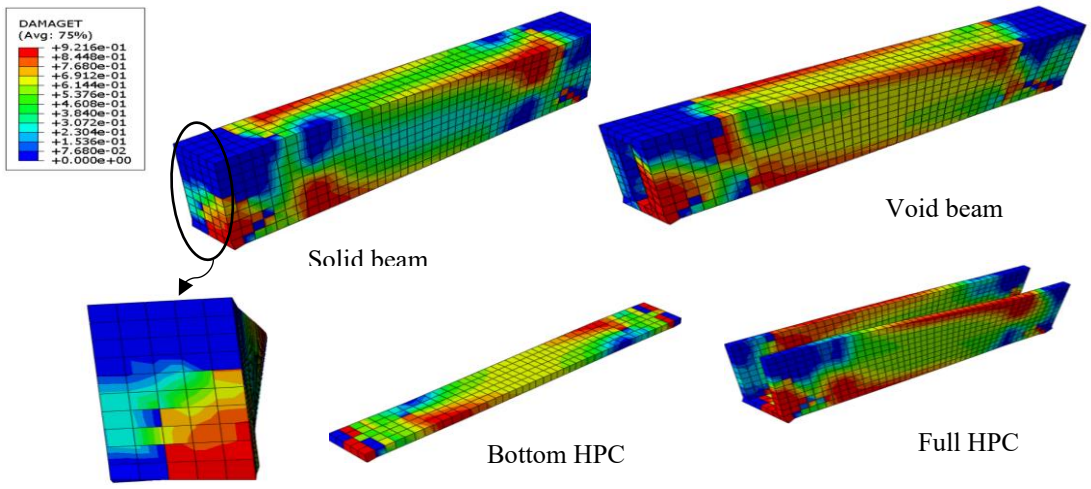

Figure 3. Torsional behavior and damage in concrete.

As the main objective of the current work is to assess the impact of strengthening reinforced concrete beams against torsional loading, the curve showing torsional moment versus twisting angle is the most comprehensive indicator for examining the effect and measuring the ability of HPC to rehabilitate such beams. Fig. 4 illustrates the torsional moment as a function of the twisting angle for the control beam and beams strengthened with different HPC techniques. Generally, the torsional moment increased gradually until reaching the peak torsional capacity, then decreased, indicating damage to the RC specimens. The maximum torsional moment was approximately 25 kN · m for the control beam. However, all strengthening methods showed higher capacity.

For the solid specimens strengthened at the bottom, the capacity showed a slight increase for twisting angles of less than 0.025 rad/m. For the beam with 50mm HPC at the bottom, the torsional moment improved by around 21%. Increasing the HPC thickness by 10mm for each specimen, up to 100mm, led to a 37% increase in torsional resistance, which is a very slight improvement, indicating an almost negligible effect of HPC on the beam resistance. Another HPC strengthening technique utilized is side rehabilitation. From the figure, adding HPC to the sides resulted in a substantial increase in torsional resistance, exceeding 80% for a beam with 50mm HPC, with a torque angle slightly exceeding 0.025 rad/m. Moreover, increasing the HPC thickness resulted in more than double the capacity compared to the control. As the HPC thickness increased to 100mm, the torsional moment increased by almost threefold, indicating meaningful improvement. The last rehabilitation method combines the first and second strengthening methods and demonstrates U-warping of the beam. The results showed that U-warping is the best method for rehabilitating the beam with HPC to increase torsion resistance. The specimen with 50mm U-warping HPC showed more than double the torsion resistance. With increasing thickness, the RC beam capacity has also been improved dramatically. When the HPC thickness was increased to 70 mm, the torsional moment increased to over 70 kN.m, highlighting the importance of strengthening the RC beam with HPC. As mentioned before, the maximum HPC thickness used in this work is 100mm, and the results indicated that the best strengthening strategy is U-shape. Thus, the maximum torsional moment achieved is about 120 kN.m, which is more than 3.5 times that of the specimen without strengthening. The outcomes also showed that U-shaped strengthening reduced the twisting angle at which maximum torque occurred, indicating reduced flexibility and making the specimens more rigid than the bare beam and other strengthening strategies. Regarding the void RC beams, the results showed that these beams exhibited lower torsional resistance than the solid beam, highlighting the importance of the beam's cross-section for overall behavior. Additionally, the work indicated that the void beam, when strengthened with HPC using different techniques, exhibited a valuable capacity enhancement similar to that of the solid beams. However, the torsional capacity of the strengthened void beams remained lower than that of the solid beams. To sum up, the solid beam is better than the void beam at resisting the applied torsional moment. Even when strengthened with U-shaped HPC, the void-beam torsional performance was still not as robust as that of reinforced-concrete solid beams.

The effect of thickness change on the peak torsion resistance of the RC beams is depicted in Fig. 5. Although the thickness

increase was the same for all rehabilitation strategies, the maximum torsion resistance varied among these strengthening methods. The solid specimens with 80mm HPC exhibited torsion values of 34.50, 62.50, and 93.30 kN · m for the bottom, sides, and full strengthening techniques, respectively. Furthermore, the beams with voids and rehabilitated with 70mm thickness showed torsional moments of 26.34, 47.00, and 62.85 kN · m for the bottom, sides, and U-shaped rehabilitation methods, respectively.

These results underscore the importance of selecting an appropriate strategy for rehabilitating the reinforced concrete beam using HPC. The stress and strain distributions on the reinforced concrete beams are shown in Fig. 6. Generally, the maximum stresses and strains occur in the middle of the RC beams, indicating torsional failure, and the materials have reached the maximum assigned values for material properties.

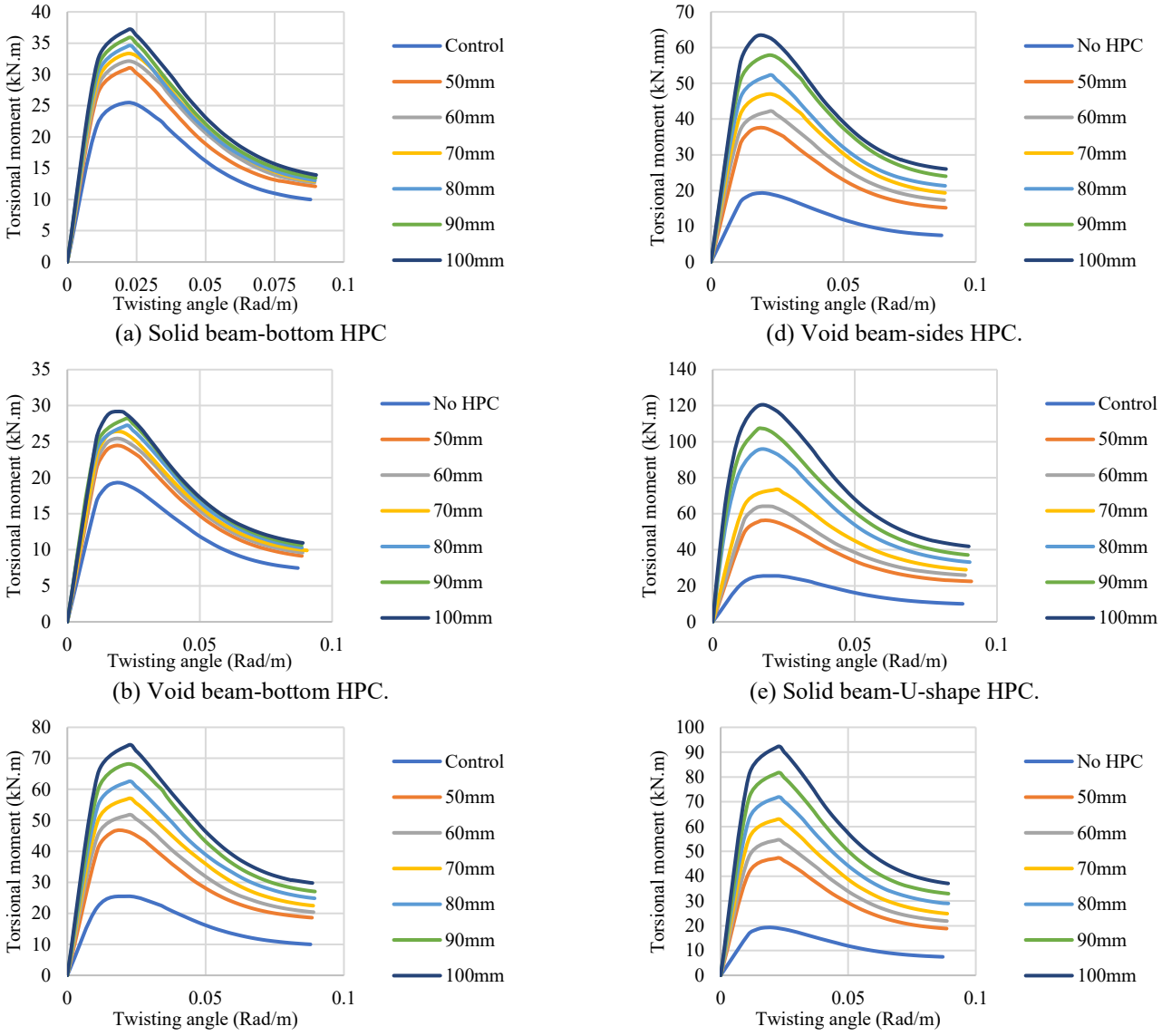

Figure 4. Torsional moment vs twisting angle for control and strengthened specimens.

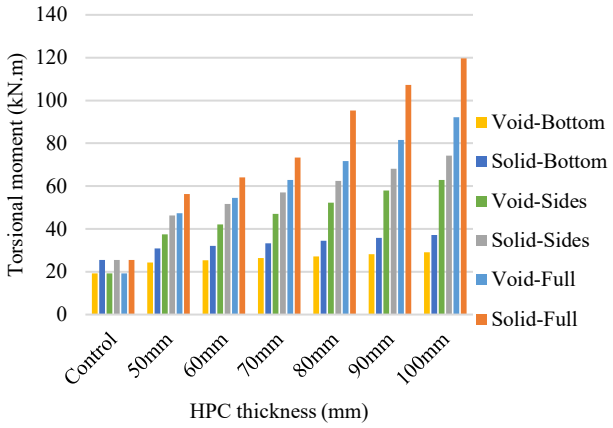

Figure 5. The effect of HPC thickness on the torsional behavior of the beam.

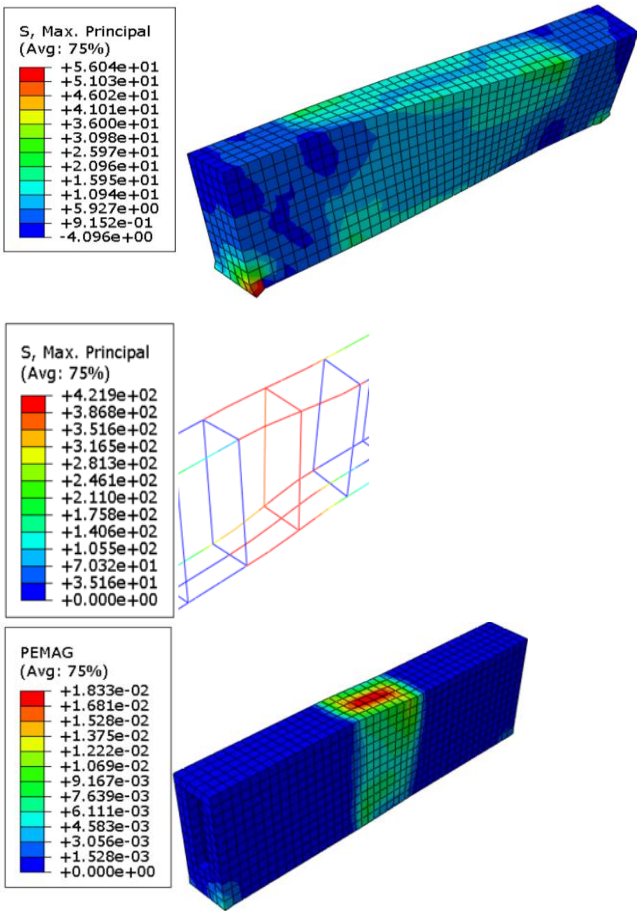

Figure 6. Stress and strain distributions on RC beam.

Fig. 7 depicts the stress-strain curve for each concrete grade. The normal concrete reached more than 30 MPa during the analysis process. However, the HPC exhibited stresses exceeding 60 MPa. These results indicate that the assigned concrete materials performed well and accurately reflected the concrete's true performance.

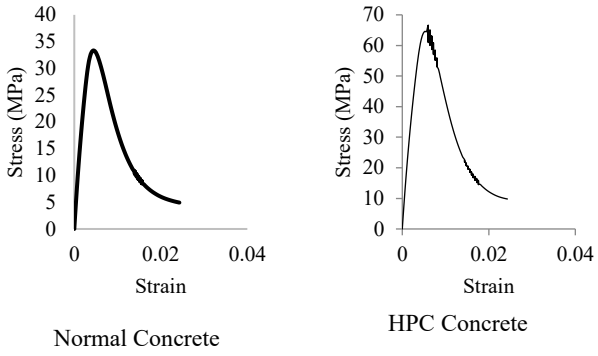

Figure 7. Stress-strain curves for both normal and high-performance concrete.

4.2 Numerical Formulation

4.2.1. Theoretical Concept

To establish a mathematical expression that accurately reflects the effect of the HPC overlay on the nominal torsional strength, the cross-section is deemed hybrid since it consists of an RC cross-section (whether solid or hollow) and an HPC overlay. Consequently, the nominal torsional strength, Tn, is equated to the torsional strength of each portion as presented in (1):

$$T_n = T_{RC} + T_{HPC} \quad (1)$$

In this equation,

T_{RC}: Torsional strength of the RC section.

T_{HPC}: Torsional strength of the HPC section.

Experimental tests reveal that solid and hollow RC cross-sections behave analogously after cracking when they have the same outside dimensions [28]. Based on this observation, the space-truss analogy method, shown in Fig. 8, can be used to determine the nominal torsional strength of the RC section, assuming that the reinforcement yields and the concrete resists no tension. This assumption leads to the equilibrium forces given by (2):

$$T_{RC} = C_1(1 - C_A)\frac{A_{oh}A_t f_{yt}}{S} \quad (2)$$

In which,

C_1: Coefficient to be determined numerically.

C_A: Ratio of void area to gross area.

A_{oh}: Area enclosed by the centreline of the stirrups.

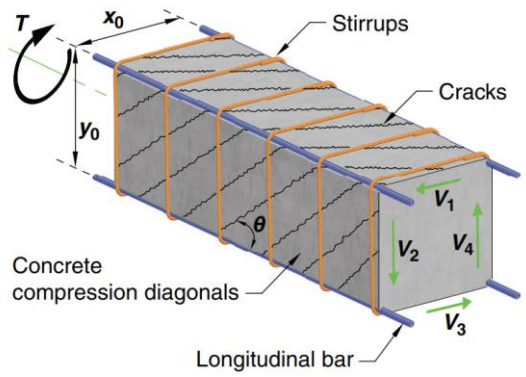

Figure 8. Space truss analogy configuration [28].

On the other hand, the HPC layer attains full resistance at the cracking torsional strength, i.e., $T_{HPC} = T_{cr}$. Diagonal cracking occurs when concrete reaches the principal tensile stress. $\left(C_2\sqrt{f_c'}\right)$, where C_2 is to be determined numerically. It is noteworthy that the ACI code conservatively takes C_2 equal to 0.33 as a lower bound value, which needs to be compared with. For elements under pure torsion, the principal tensile stress is equated to the torsional shear stress as shown in (3):

$$T_{HPC} = C_3\sqrt{f_c'}L_m t^2 \quad (3)$$

In which,

$C_3 = 1.7C_2$

L_m: Length of the HPC layer's centreline.

t: Thickness of the HPC layer.

Now, substituting (2) and (3) into (1) gives the nominal torsional strength of the hybrid cross-section as formulated in (4):

$$T_n = C_1(1 - C_A)\frac{A_{oh}A_t f_{yt}}{s} + C_3\sqrt{f_c'}L_m t^2 \quad (4)$$

4.2.2. Numerical Concept

Multiple linear regression analysis at the 95% confidence level has been used to estimate the coefficients of the torsional strength equation based on the FE analysis results. To this end, trials have been conducted on the entire dataset to determine the most representative values, including torsional strengths and corresponding properties, as presented in Tables 4 and 5, before comparison with ACI values.

Subsequently, accurate arithmetic operations were performed to compute the coefficients of the independent variables in the equation for total torsional strength, as detailed in Table 6, along with the correlation results. As a consequence, the statistical data were assessed using the coefficient of determination (R^2), which was employed in the present work to evaluate the performance of the developed models.

Conclusively, both analyses exhibited a strong fit with regard to the influential independent variables. Therefore, the equation representing the relationship between torsional strengths and the corresponding thickness of the HPC layer can be expressed as defined in (5) and (6) for the solid and void beams, respectively:

$$T_n = 1.42\frac{A_{oh}A_t f_{yt}}{s} + \sqrt{0.5f_c'}L_m t^2 \quad (5)$$

$$T_n = 1.82(1 - Av/Ag)\frac{A_{oh}A_t f_{yt}}{s} + 0.6\sqrt{f_c'}L_m t^2 \quad (6)$$

Furthermore, the principal tensile stress can be determined from (7) using the average values of C2, yielding a higher percentage of 15.2% than the value stipulated in the ACI code, thus indicating a significant deviation from the standard recommendation.

$$f_t = 0.38\sqrt{f_c'} \quad (7)$$

Table 4. Input parameters for formulating torsional strengths of solid beams.

Nominal Torsional Strength, T_i, kN.mm				HPC layer	
TNC	TB	TRL	TRBL	t^2, mm²	L_m, mm TB/TRL/TRBL
	25495.74	25495.74	25495.74	0	0/0/0
	30968.67	46334.36	56313.70	2500	300/1200/1600
	32122.32	51700.97	64075.35	3600	300/1200/1620
25495.74	33340.03	56981.49	73405.67	4900	300/1200/1640
	34550.73	62456.93	95324.86	6400	300/1200/1660
	35827.98	68189.04	107305.76	8100	300/1200/1680
	37149.53	74198.38	119746.81	10000	300/1200/1700

Table 5. Input parameters for formulating torsional strengths of void beams.

Nominal Torsional Strength, T_i, kN.mm				HPC layer	
T_{NC}	T_B	T_{RL}	T_{RBL}	t^2, mm^2	L_m, mm $T_B/T_{RL}/T_{RBL}$
	19247.85	19247.85	19247.85	0	0/0/0
	24366.47	37437.61	47266.95	2500	300/1200/1600
	25326.94	42160.66	54548.55	3600	300/1200/1620
19247.85	26345.70	47016.98	62856.88	4900	300/1200/1640
	27209.21	52237.38	71749.30	6400	300/1200/1660
	28167.27	57893.26	81559.03	8100	300/1200/1680
	29163.09	62815.46	92107.54	10000	300/1200/1700

Table 6. Regression statistics output for the solid and void beams.

Beam type	T_n	Terms	Coefficients	P-value	Standard Error	Multiple R	R^2
Solid beams	T_s	C_1	1.42	-	0	1.0000	1.0000
		C_2	0.42*			-	
		C_3	$1/\sqrt{2}$	3.9E-15	0.027	0.9876	0.9754
		C_A	0			-	
Void beams	T_v	C_1	1.82	-	0	1.0000	1.0000
		C_2	0.34*			-	
		C_3	0.58	1.1E-15	0.021	0.9894	0.9790
		C_A	Av/Ag			-	

*$C_2 = C_3/1.7$

4.3. Verification between Formulation and FE Results

Six strengthened beams with a cross-section of 250 × 500 mm and the same adopted reinforcement were utilized to verify the numerical formulation against FE results, ensuring that the computational models accurately reflect the expected structural behavior. This comparison is crucial for validating the FEM simulations, building confidence in the numerical predictions, and potentially highlighting areas for refinement in the ACI code and the numerical model. Moreover, it enables assessment of the reliability and applicability of the FEM for predicting the torsional response of reinforced concrete beams. The comparison results, along with the percentage variations, are presented in Table 7.

The results in Table 7 generally indicate good agreement between the numerical nominal torsion and FE results for the selected beams. It can also be observed that the numerical results are consistently lower than the FE results, with variation percentages ranging from -2.4% to -7.3%. This indicates that the numerical formulation is closer to the FEM simulations.

Moreover, to assess the performance of the predicted equation, two additional RC beams strengthened with HPC were modeled in ABAQUS, using the properties of the control beams as test data for the adopted equation. The first beam model was a solid beam strengthened with a 74mm U-shaped HPC, and the second model was a void beam strengthened with a 76mm U-shaped HPC. The numerical simulation results are shown in Fig. 9. The FE results indicated a comprehensive performance of HPC by improving the torsional capacity of RC beams. The maximum torsional moments recorded were 80 and 67 kN.m for the solid and void beams, respectively. In contrast, the numerical equation gave lower values by about 6.2% for the solid beam and 7.7% for the void beam, indicating good prediction and that it can be relied on for practical applications in design and analysis. The slight underestimation by the numerical model suggests a conservative approach. Further refinement of the numerical model may yield even closer alignment with the FE results, enhancing the predictive capability of the proposed equation.

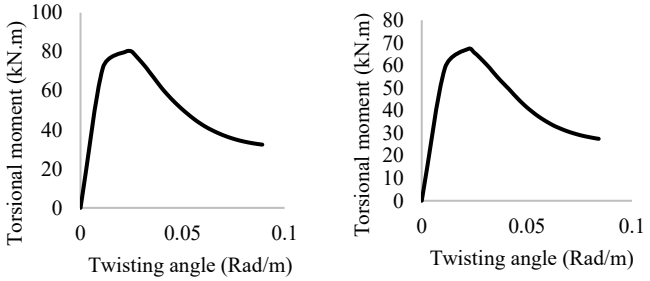

(a)Solid U-shaped 74mm HPC (b) Void U-shaped 76mm HPC

Figure 9. Torsional moment vs twisting angle for selected testing data.

Table 7. Comparison of numerical nominal torsion and FE results.

Beam ID		Numerical results (5) or (6) kN.mm	FE results kN.mm	Variation* %
Solid	B-110	45,464.90	47,057.56	-3.4
	RL-85	56,313.89	60,719.21	-7.3
	RBL-120	134,248.52	141,315.31	-5.0
Hollow (void: 300×50)	B-110	31,303.39	33,088.24	-5.4
	RL-85	54,304.26	55,627.18	-2.4
	RBL-120	132,238.89	136,837.39	-3.4

*The (-ve) sign indicates that the numerical results are less than the FE results.

5. Conclusions

In the present paper, a numerical analysis was conducted to explore the torsional behavior of reinforced concrete beams, further enhanced by the use of high-performance concrete. The findings suggest that high-performance concrete is effective in reinforcing beams under torsion due to its high strength and its positive correlation with shear stresses. Among various strengthening techniques, the U-shaped method emerged as the most effective, delivering the greatest improvement in torsional performance, particularly at locations where torsional stresses are highest. Solid RC beams outperformed hollow RC beams by approximately 32% in torsional resistance, due to core confinement. Both solid and hollow beams exhibited significant improvements in torsional performance upon strengthening. The finite element method proved to be a robust approach for simulating RC beams and achieving the desired performance. On the other hand, the numerical formulation, based on the space truss analogy method - akin to the one adopted by the ACI code but with statistically determined coefficients - yielded high R^2 values, indicating a reliable predictive model for torsional strength. Notably, the average C2 utilization was 15.2% higher than the conservative ACI code estimates, suggesting the possibility of more efficient design parameters. The constitutive model effectively validated the numerical results, with a maximum discrepancy of only 7% compared to the FEM results, underscoring the model's accuracy. Further experimental tests and numerical analyses are recommended, as well as the implementation of strengthening techniques and the use of highly ductile concrete.

Acknowledgements

The authors would like to express their appreciation for the constructive feedback from colleagues and the resources provided. The authors are also grateful for the support from the Department of Civil Engineering at the University of Warith Al-Anbiyaa.

Conflict of interest

The authors declare that there are no conflicts of interest regarding the publication of this manuscript.

Author Contribution Statement

Maher K. Abbas designed the conceptualization, methodology, numerical formulation, and discussion.

Mustafa Kareem Hamzah conducted FE analysis, validation, and discussion.

Zahraa A. Naser collected references and the introduction.

Nabeel H. Al-Salim contributed to the conceptualization and provided methodology.

References

[1] A. A. Hamoda, B. A. Eltaly, M. Ghalla, and Q. Q. Liang, "Behavior of reinforced concrete ring beams strengthened with sustainable materials," *Engineering Structures*, vol. 290, no. 116374, 2023. doi: https://doi.org/10.1016/j.engstruct.2023.116374.

[2] S. H. Muhammed and A. H. Aziz, "Torsion Enhancement of Reinforced Self-Compacting Concrete Box Beams Using Internal Framed Steel Stiffening Ribs," *J. Eng. Sustain. Dev.*, vol. 24, no. 4, pp. 89–103, 2020 . doi: https://doi.org/10.31272/jeasd.24.4.10

[3] M. L. Wang and D. Keierleber, "Investigation of shear strength of SIFCON using torsion tests," *Construction and Building Materials*, vol. 5, no. 2, pp. 93–100, 1991, doi: https://doi.org/10.1016/0950-0618(91)90007-8

[4] M. I. Ali and A. A. Al-Azzawi, "Finite element analysis of RC beams strengthened with near-surface mounted reinforcement bars under pure torsion," *IOP Conference Series: Earth and Environmental Science*, vol. 1232, no. 1, no. 012026, 2023. doi: https://doi.org/10.1088/1755-1315/1232/1/012026.

[5] A. R. Zojaji and M. Z. Kabir, "Analytical approach for predicting full torsional behavior of reinforced concrete beams strengthened with FRP materials," *Sci. Iran.*, vol. 19, no. 1, pp. 51–63, 2012. doi: https://doi.org/10.1016/j.scient.2011.12.004

[6] R. S. Atea, "Torsional Behavior of Reinforced Concrete T Beams Strengthened with CFRP Strips," *Case Stud. Constr. Mater.*, vol. 7, no. March, pp. 110–117, 2017. doi: https://doi.org/10.1016/j.cscm.2017.03.002.

[7] S. B. Kandekar and R. S. Talikoti, "Torsional behaviour of reinforced concrete beam wrapped with aramid fiber," *J. King Saud Univ. - Eng. Sci.*, vol. 31, no. 4, pp. 340–344, 2019. doi: https://doi.org/10.1016/j.jksues.2018.02.001.

[8] G. C. Behera, T. D. G. Rao, and C. B. K. Rao, "Torsional behaviour of reinforced concrete beams with ferrocement U-jacketing-Experimental study," *Case Stud. Constr. Mater.*, vol. 4, pp. 15–31, 2016. doi: https://doi.org/10.1016/j.cscm.2015.10.003.

[9] M. Abdel-Ghaffar, A. Salah-Eldin, A. Erfan, and A. Salem, "Experimental investigation of fibrous reinforced concrete beams under torsion loads," *Engineering Research Journal - Faculty of Engineering (Shoubra)*, vol. 52, no. 2, pp. 172–176, 2023. doi: https://doi.org/10.21608/erjsh.2023.191020.1138.

[10] M. A. El-Mandouh, J.-W. Hu, W.-S. Shim, F. Abdelazeem, and G. Elsamak, "Torsional improvement of RC beams using various strengthening systems," *Buildings*, vol. 12, no. 11, no. 1776, 2022. doi: https://doi.org/10.3390/buildings12111776

[11] T. J. Mohammed, B. H. Abu Bakar, and N. M. Bunnori, "Effects of

thickness of ultra-high-performance fiber concrete wrapping on the torsional strength of reinforced concrete beam," *Applied Mechanics and Materials*, vol. 802, pp. 161–165, 2015. doi: https://doi.org/10.4028/www.scientific.net/AMM.802.161.

[12] C. Zhou, J. Wang, X. Shao, L. Li, J. Sun, and X. Wang, "The feasibility of using ultra-high performance concrete (UHPC) to strengthen RC beams in torsion," *J. Mater. Res. Technol.*, vol. 24, pp. 9961–9983, 2023. doi: https://doi.org/10.1016/j.jmrt.2023.05.185

[13] A. P. Lampropoulos, S. A. Paschalis, O. T. Tsioulou, and S. E. Dritsos, "Strengthening of existing reinforced concrete beams using ultra high performance fibre reinforced concrete," in *Concrete Repair, Rehabilitation and Retrofitting IV: Proc. 4th Int. Conf. on Concrete Repair, Rehabilitation and Retrofitting (ICCRRR 2015)*, Leipzig, Germany, 2015, pp. 124–125. doi: https://doi.org/10.1201/b18972-80.

[14] P. R. Prem and A. R. Murthy, "Acoustic emission and flexural behaviour of RC beams strengthened with UHPC overlay," *Constr. Build. Mater.*, vol. 123, pp. 481–492, 2016. doi: https://doi.org/10.1016/j.conbuildmat.2016.07.033.

[15] M. Safdar, T. Matsumoto, and K. Kakuma, "Flexural behavior of reinforced concrete beams repaired with ultra-high performance fiber reinforced concrete (UHPFRC)," *Compos. Struct.*, vol. 157, pp. 448–460, Dec. 2016. doi: https://doi.org/10.1016/j.compstruct.2016.09.010.

[16] J. K. Mures, M. A. I. Ahmed, and A. H. Chkheiwer, "Torsional behavior of high strength concrete members strengthened by mixed steel fibers," *Journal of Engineering*, vol. 2021, no. 5539623, 2021. doi: https://doi.org/10.1155/2021/5539623.

[17] R. Ullah, Y. Qiang, J. Ahmad, N. I. Vatin, and M. A. El-Shorbagy, "Ultra-high-performance concrete (UHPC): A state-of-the-art review," *Materials*, vol. 15, no. 12, no. 4131, 2022. doi: https://doi.org/10.3390/ma15124131.

[18] A. Karimipour, J. de Brito, M. Ghalehnovi, and O. Gençel, "Torsional behaviour of rectangular high-performance fiber-reinforced concrete beams," *Structures*, vol. 35, pp. 511–519, 2022. doi: https://doi.org/10.1016/j.istruc.2021.11.037

[19] N. Ayaad and N. Oukaili, "Impact torsional behavior and strengthening of reinforced concrete spandrel beams," *Case Stud. Constr. Mater.*, vol. 19, no. October, p. e02591, 2023. doi: https://doi.org/10.1016/j.cscm.2023.e02591.

[20] T. J. Mohammed, K. M. Breesem, and A. F. Hussein, "Numerical analysis of torsional reinforcement of concrete beams in unconventional by ANSYS software," *Civil Engineering Journal*, vol. 9, no. 1, pp. 41–51, Jan. 2023. doi: https://doi.org/10.28991/CEJ-2023-09-01-04.

[21] A. G. Nasser, M. H. *Makhlouf*, K. M. Elsayed, and G. I. K., "Experimental and numerical investigation on RC beams with web openings subjected to pure torsion strengthened by ferrocement technique or GFRP sheets," *Structures*, vol. 69, Art. no. 107479, Nov. 2024, doi: https://doi.org/10.1016/j.istruc.2024.107479

[22] M. A. Alrawi and M. N. Mahmood, "Torsional Behavior of Strengthened Reinforced Concrete Beams by CFRP Sheets: Parametric study," *Anbar J. Eng. Sci.*, vol. 12, no. 2, pp. 229–244, 2021. doi: https://doi.org/10.37649/aengs.2021.171191.

[23] X. Chen, Z. Wang, **et al.**, "Torsional strengthening using carbon fiber reinforced polymer of reinforced concrete beams subject to combined bending, shear and torsion," *Advances in Structural Engineering*, vol. 26, no. 2, pp. 272-286, 2023, doi: https://doi.org/10.1177/13694332221124624.

[24] T. J. Mohammed, B. H. A. Bakar, and N. M. Bunnori, "Torsional improvement of reinforced concrete beams using ultra high-performance fiber reinforced concrete (UHPFC) jackets – Experimental study," *Constr. Build. Mater.*, vol. 106, pp. 533–542, 2016. doi: https://doi.org/10.1016/j.conbuildmat.2015.12.160.

[25] X. Cao, L. Wu, and Z. Li, "Behaviour of steel-reinforced concrete columns under combined torsion based on ABAQUS FEA," *Engineering Structures*, vol. 209, no. 109980, 2020. doi: https://doi.org/10.1016/j.engstruct.2019.109980.

[26] B. Eltaly, M. El-Sayed, N. Meleka, and K. Kandil, "Torsion behavior of strengthened reinforced concrete box girders with openings: Analytical and experimental investigation," *Structures*, vol. 60, Art. no. 105908, Feb. 2024. doi: https://doi.org/10.1016/j.istruc.2024.105908.

[27] M. K. Abbas and M. K. Hamzah, "Numerical investigation on flexural performance of hybrid concrete T-beams," in *AIP Conference Proceedings*, vol. 2806, no. 1, no. 040041, 2023. doi: https://doi.org/10.1063/5.0166265.

[28] ACI Committee 318, *Building Code Requirements for Structural Concrete (ACI 318-19) and Commentary*. Farmington Hills, MI, USA: American Concrete Institute, 2019. [Online]. Available: https://www.concrete.org/store/productdetail.aspx?ItemID=318U19.